

Nonpolar $\text{In}_x\text{Ga}_{1-x}\text{N}/\text{GaN}(1\bar{1}00)$ multiple quantum wells grown on $\gamma\text{-LiAlO}_2(100)$ by plasma-assisted molecular-beam epitaxy

Yue Jun Sun,* Oliver Brandt, Sven Cronenberg, Subhabrata Dhar, Holger T. Grahn, and Klaus H. Ploog
Paul-Drude-Institut für Festkörperelektronik, Hausvogteiplatz 5–7, D-10117 Berlin, Germany

Patrick Waltereit and James S. Speck

Materials Department, University of California, Santa Barbara, California 93106

(Received 9 September 2002; published 30 January 2003)

M-plane $\text{In}_{0.1}\text{Ga}_{0.9}\text{N}(1\bar{1}00)$ multiple quantum wells were grown on $\gamma\text{-LiAlO}_2(100)$ by plasma-assisted molecular-beam epitaxy. The high brightness of the photoluminescence of these multiple quantum wells and the observation of band-edge emission from the barriers are consistent with the expected absence of spontaneous and piezoelectric polarization fields along the growth direction. Despite this fact, the recombination dynamics observed is rather complex and is shown to originate from the superposition of exciton relaxation towards a band of localized states and simultaneous recombination.

DOI: 10.1103/PhysRevB.67.041306

PACS number(s): 72.20.Jv, 78.55.Cr, 78.67.De, 81.15.Hi

Very recently, the interest in nonpolar group-III nitride heterostructures has increased remarkably.^{1–3} The reason for this surge of activity is the absence of internal electrostatic fields in these structures, unlike in conventional *C*-plane ([0001]-oriented) structures, where these fields inevitably reduce the internal quantum efficiency. Nonpolar GaN/(Al,Ga)N multiple quantum wells (MQW's) have been realized, either grown on $\gamma\text{-LiAlO}_2(100)$ [LAO(100)] (Ref. 4) or on *R*-plane ($1\bar{1}02$) sapphire.¹ However, nonpolar (In,Ga)N/GaN MQW's have not been synthesized yet. Our previous attempt produced a predominantly *C*-plane structure because of the inappropriate nucleation conditions.⁵ Here, we employ a low-temperature GaN instead of an AlN nucleation layer, resulting in pure *M*-plane growth.

In this Rapid Communication, we report on the growth of *M*-plane (In,Ga)N/GaN MQW's on LAO(100) and a detailed investigation of their structural and optical properties. We have fabricated a number of structures with different In content (5–10%) and well width (2–4 nm), which exhibit emission energies between 3.0 and 3.35 eV. In contrast to the GaN/(Al,Ga)N MQW's studied in our previous work,⁴ the recombination dynamics observed for all of the present $\text{In}_{0.1}\text{Ga}_{0.9}\text{N}/\text{GaN}$ MQW's is nonexponential and significantly slower than expected for free excitons. Focusing on one exemplary sample, we provide various indications for the absence of internal electrostatic fields in these MQW's. The complex photoluminescence decay observed is attributed to the presence of localized states.

The (In,Ga)N/GaN MQW's were grown on LAO(100) by rf plasma-assisted molecular-beam epitaxy, equipped with reflection high-energy electron diffraction (RHEED) for *in situ* monitoring of the growth. The as-received $1 \times 1 \text{ cm}^2$ LAO substrates were degreased with organic solvents and dipped briefly (30 s) in deionized water. Next, the LAO substrate was soldered onto a Si wafer with In, which is clipped to a Mo holder. Prior to growth, the substrate was outgassed in the load-lock chamber for 1 h at 200 °C. Growth was initiated at 660 °C and Ga-rich conditions for the first 70 nm of GaN, after which the temperature was increased to 750 °C

for the remaining 500 nm. Note that a low-temperature and Ga-rich nucleation stage is crucial for obtaining pure *M*-plane GaN films.⁶ For the deposition of the (In,Ga)N/GaN MQW, the substrate temperature was lowered to 610 °C. Ga-stable conditions were used for the buffer layer and slightly N-rich conditions for the MQW. The RHEED pattern was entirely streaky along the $[1\bar{1}\bar{2}0]$, but modulated along the [0001] azimuth. Indeed, atomic force micrographs (not shown here) display a highly anisotropic surface morphology with smooth stripes running along the $[1\bar{1}\bar{2}0]$ direction. The peak-to-valley roughness amounts to 30 nm over $3 \times 3 \mu\text{m}^2$, and the rms roughness is 3.7 nm over the same area. The samples were then analyzed by high-resolution x-ray diffraction, continuous-wave (cw) and time-resolved photoluminescence (PL) spectroscopy. Symmetric x-ray ω - 2θ scans were taken with a Philips X'Pert PRO triple-axis diffractometer equipped with a Cu $K\alpha_1$ source in the focus of a multilayer x-ray mirror, a four-bounce Ge(022) monochromator in dispersive configuration, and a two-bounce Ge(022) analyzer. Cw-PL spectra at various temperatures were recorded using a 325-nm He-Cd laser with an excitation intensity of 10 W/cm². Time-resolved PL (TRPL) measurements at 7 K and at various excitation fluences were performed with a frequency-doubled Ti:sapphire laser with a photon energy of 3.4 eV, a pulse width of about 200 fs, and a repetition rate of 4.75 MHz. For detection, a Hamamatsu C5680 streak camera was used.

Figure 1 shows an ω - 2θ scan for the 20-period $\text{In}_{0.1}\text{Ga}_{0.9}\text{N}/\text{GaN}$ MQW we will focus on in this paper. The nominal structural parameters of this MQW, extracted from previous runs on SiC(0001), are well and barrier thicknesses of 2 and 7 nm, respectively, and an In content of 15%. Several important conclusions can be drawn from this scan.

(i) No additional signal is detected at the position of either GaN(0002) or in between GaN(0002) and $\text{In}_{0.1}\text{Ga}_{0.9}\text{N}(0002)$, demonstrating that the entire structure has the expected orientational relationship, i.e., $[1\bar{1}\bar{0}0]_{(\text{In,Ga})\text{N}} \parallel [100]_{\text{LAO}}$. Additional resonant Raman

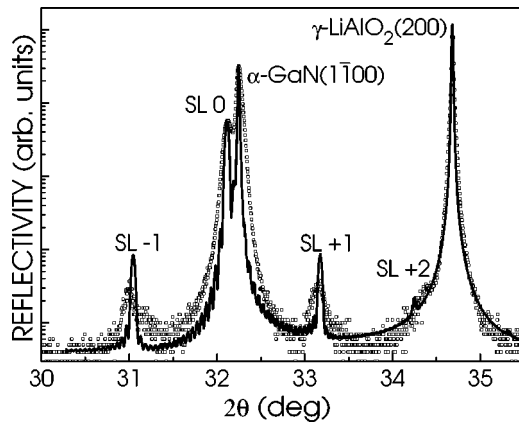


FIG. 1. Experimental (\square) and simulated ($—$) triple-axis ω - 2θ scan across the GaN($1\bar{1}00$) reflection of a 20-period $\text{In}_{0.1}\text{Ga}_{0.9}\text{N}/\text{GaN}$ MQW grown on LAO(100). The superlattice satellites are denoted by $\text{SL}\pm n$. The simulation is normalized to the GaN ($1\bar{1}00$) reflection to account for the mosaicity of the layers.

measurements (not shown here) demonstrate that the structure also fulfills the expected in-plane orientation relationship, namely, $[0001]_{(\text{In,Ga})\text{N}}\parallel[010]_{\text{LAO}}$ and $[11\bar{2}0]_{(\text{In,Ga})\text{N}}\parallel[001]_{\text{LAO}}$.

(ii) The angular separation between the LAO(200) and GaN($1\bar{1}00$) reflections indicates a lattice dilation of 0.63% along the growth direction, i.e., $[1\bar{1}00]$, for the GaN buffer. This fairly high strain is at least partly a result of the coherent growth of GaN($1\bar{1}00$) on LAO(100) along the $[0001]$ direction,⁷ where the lattice mismatch amounts to only 0.3%. The mismatch in thermal expansion, of course, is also compressive and enhances this effect.

(iii) First-order superlattice satellites are observed, demonstrating the periodicity of the structure and allowing us to determine its structural parameters. A kinematical analysis⁸ yields well and barrier thicknesses of 1.9 nm and 6.6 nm, respectively, and an In content of 10%. The simulation based on dynamical diffraction theory, an exact incidence parameter,⁸ and these kinematically obtained parameters is seen to agree with the experiment (cf. Fig. 1) in view of the angular positions of the reflections. A significant broadening is observed, however, for the experimental data, particularly so for the higher-order satellites. This broadening is at least partially caused by inhomogeneous strain (cf. SL 0 in Fig. 1), but also by interface roughness.

It is important to note that these data do not allow us to discriminate between different spatial distributions of the In content for the lack of higher-order satellites and the broadening of the lower-order satellites.^{8,9} We thus cannot detect whether or not In surface segregation plays an essential role here.

Figure 2 shows the evolution of the cw PL spectra from 5 to 300 K for the sample under investigation. The dominant emission centered at 3.13 eV stems from the $\text{In}_{0.1}\text{Ga}_{0.9}\text{N}/\text{GaN}$ MQW. Interestingly, we also observe emission at 3.36 eV originating from excitons bound to stacking faults in GaN,¹⁰ and at 3.499 eV from the (D^0, X) transition in GaN. The energy position of the latter indicates a large

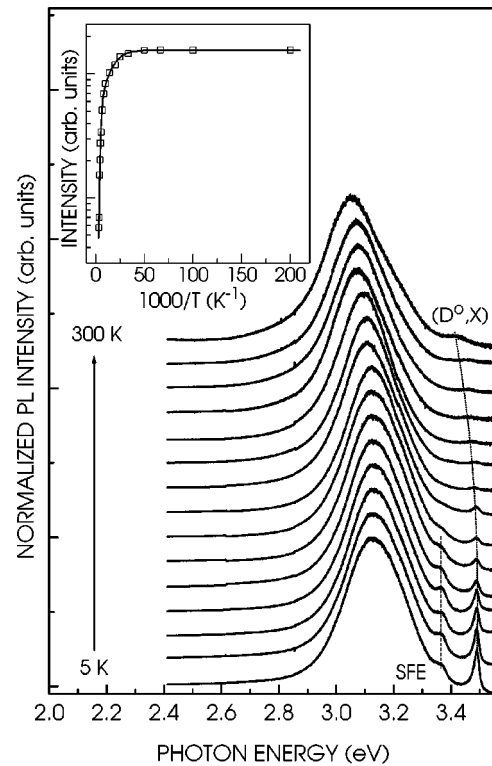


FIG. 2. PL spectra of the M -plane $\text{In}_{0.1}\text{Ga}_{0.9}\text{N}/\text{GaN}$ MQW in the temperature range from 5 K to 300 K. All spectra are normalized and vertically offset for clarity. The inset shows an Arrhenius representation of the integrated PL intensity. The solid line is a fit using the standard formula $I(T)/I_0 = [1 + c_1 \exp(-E_{a1}/kT) + c_2 \exp(-E_{a2}/kT)]^{-1}$, where E_{a1} and E_{a2} are the thermal activation energies and c_1 and c_2 are the weights of the respective non-radiative dissociation channels. The fit returns activation energies E_{a1} and E_{a2} of 11 meV and 95 meV, respectively.

compressive strain,^{11,12} which is consistent with the x-ray-diffraction measurements described above. However, the observation of luminescence from GaN alone is interesting, since we never detected any signal from GaN in the case of C -plane $\text{In}_{0.1}\text{Ga}_{0.9}\text{N}/\text{GaN}$ MQW's with a total thickness, as the present sample, exceeding the penetration depth of the laser. The lack of GaN luminescence in that case is plausible: the internal electrostatic fields in the barriers of C -plane $\text{In}_{0.1}\text{Ga}_{0.9}\text{N}/\text{GaN}$ MQW's rapidly separate electrons and holes and direct them to the wells, thereby enhancing the capture efficiency. The observation of rather strong luminescence from the GaN barriers in the present sample may thus be taken as a manifestation of the absence of internal electrostatic fields.

A quantitative comparison of the transition energy is, in contrast to our previous investigation of GaN/(Al,Ga)N MQW's,⁴ difficult for the following reasons. Surface segregation of In, if present, may strongly distort the intended compositional profile and result in a large blueshift of the transition.¹³ Compositional fluctuations, on the other hand, will lead to a redshift. Finally, the biaxial strain within the $\text{In}_{0.1}\text{Ga}_{0.9}\text{N}$ wells is inherently anisotropic and affects the band structure in a more complex way than the isotropic biaxial strain in C -plane structures.¹⁴ Neglecting these com-

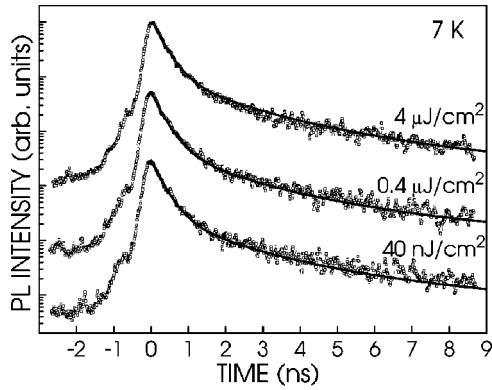


FIG. 3. Integrated TRPL intensity transients at three different excitation fluences as indicated in the figure for the M -plane $\text{In}_{0.1}\text{Ga}_{0.9}\text{N}/\text{GaN}$ MQW under investigation. Open circles are the experimental data, solid lines show fits with identical parameters except for the amplitude, as described in the text. The apparent step in the data prior to the pulse is an experimental artifact.

plications and assuming that piezopolarization and spontaneous polarization in this M -plane structure are absent, i.e., the MQW has a “flat band” profile, we obtain a transition energy of 3.13 eV. This exact agreement with the experimental value is of course fortuitous, as we would expect the actual transition energy to be lower by the exciton binding energy and, as we will see below, the energy of localized states. It is thus likely that In surface segregation occurs just as in the case of C -plane $(\text{In,Ga})\text{N}$ MQW’s,^{9,13} and causes a higher transition energy than theoretically anticipated. However, we found that the PL transition energies from similar structures with wider wells seem to depend solely on the In content in the well and *not* on the quantum well width, which provides another indication of the absence of internal fields in these structures. Still, it is evident that a direct proof for the presence or absence of internal electrostatic fields in the present structures is considerably more difficult than in $\text{GaN}/(\text{Al,Ga})\text{N}$ MQW’s, where neither surface segregation nor compositional fluctuations (both of which might even depend on the In content) need to be considered.

The inset of Fig. 2 shows an Arrhenius plot of the integrated cw PL intensity of the MQW. The total PL intensity of the M -plane MQW is reduced by a factor of 25 when the temperature is increased from 5 to 300 K. Beyond 70 K, the luminescence is thermally quenched with an activation energy of about 95 meV. Still, this MQW’s PL intensity ranks highest among our samples and those we have obtained from other groups (including samples fabricated by metal-organic vapor phase epitaxy), particularly so at room temperature.

Figure 3 shows TRPL transients after the excitation of the wells only with different excitation fluences. The initial decay is rapid, faster than that we have observed for C -plane MQW’s with similar structural parameters. The transients, however, cannot be fitted by either a biexponential or a stretched exponential.^{15–20} It is worth noting that the transients exhibit an identical behavior for different excitation fluences. This finding is in complete contrast to C -plane MQW’s, where screening of the electric field occurs at these carrier densities (10^{18} cm^{-3}), and as such provides a further

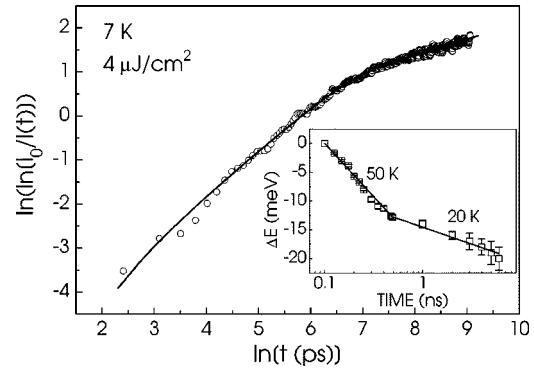


FIG. 4. Double log-log representation of the PL transient obtained with the excitation fluence as indicated. Open circles are the experimental data, solid line shows the fit. The inset illustrates the spectral diffusion of the PL band. Note the different slopes for short and long times. The solid lines in the inset are fits according to the equation $\Delta E = -kT_{ac} \ln(\nu t)$.

sign for the actual absence of internal electrostatic fields.

Figure 4 shows the transient obtained with the highest excitation fluence plotted as $\ln[\ln(I_0/I(t))]$ vs $\ln(t)$, in which a stretched exponential would be a straight line. Obviously, the data cannot be represented by a stretched exponential. The key for understanding the recombination dynamics for this sample is displayed in the inset of Fig. 4. The PL band exhibits rapid spectral diffusion during the first 500 ps after excitation. For longer time, the PL band still redshifts, but significantly slower.

We interpret this finding as follows: following excitation at 3.4 eV, the photogenerated excitons thermalize and initially occupy extended states in the QW. These free excitons then rapidly relax towards lower-lying localized states, which is the reason for the rapid spectral diffusion as well as for the rapid initial decay of the PL transient. Once reaching the localized states, the excitons are subject to a much slower redistribution within the band of localized states, described by a stretched exponential.¹⁵ Mathematically, we thus deal with the following situation:

$$\frac{dn_f(t)}{dt} = G(t) - \frac{n_f(t)}{\tau_f} - \frac{n_f(t)}{\tau_r}, \quad (1)$$

$$\frac{dn_b(t)}{dt} = \frac{n_f(t)}{\tau_r} - t^{\beta-1} \frac{n_b(t)}{\tau_b}, \quad (2)$$

where $G(t)$ is the excitation pulse, n_f and n_b are the densities of free and bound excitons, respectively, τ_f and τ_b are the corresponding radiative lifetimes, τ_r is the relaxation time, and β is the dimensionality parameter. This rate-equation system has no analytical solution, but we have found that the sum of an exponential [$\propto \exp(-t/\tau_r')$, representing the relaxation from free excitons towards localized states with $1/\tau_r' = 1/\tau_f + 1/\tau_r$] and a stretched exponential [$\propto \exp(-t/\tau_b')^{\beta'}$, accounting for the slow communication between the localized states] is a sensible approximation, although the values for the individual lifetimes and the dimensionality parameter β are then modified. The fits shown in

Figs. 3 and 4 were made with identical parameters (except, of course, for the amplitude), namely, $\tau_r' = 0.2$ ns, $\tau_b' = 1$ ns, $\beta' = 0.68$. The former value is a superposition of both relaxation and radiative recombination of free excitons, and thus cannot be decomposed. The latter parameters, however, roughly correspond to $\tau_b = 3$ ns and $\beta = 0.5$ as judged from our numerical simulations of Eqs. (1) and (2). These are similar values as found for nonpolar cubic (In,Ga)N.^{20,21}

Finally, it is interesting to note that the energy shift displayed in the inset of Fig. 4 is logarithmic in nature and can be described by $\Delta E = -kT_{ac} \ln(\nu t)$, with the acoustic-phonon temperature T_{ac} and the attempt-to-escape rate $\nu \approx 10^{12}$ s⁻¹. This logarithmic relaxation has been observed before, both for the case of multiple-trapping relaxation of carriers within a band of localized states²² and for relaxation of excitons towards localized states in quantum wells.²³ The temperatures required to fit our data are found to be significantly higher than the actual lattice temperature, namely, 50 K for the short-time region and 20 K for the long-time region. This behavior is identical to that observed by Göbel and Graudszus,²² and has been attributed to the fact that the relaxation process itself proceeds by the generation of phonons, thus increasing the phonon population over the thermal equilibrium value. In this context, the difference of the phonon temperatures extracted from our experiments is

easy to understand: while the relaxation of free excitons towards localized states proceeds exclusively by the generation of phonons, excitons—once occupying localized states—have to rely at least partly on existing phonons to assist them to migrate within the band of localized states.

In conclusion, we have shown that the synthesis of *M*-plane In_{0.1}Ga_{0.9}N/GaN MQW's is feasible. These structures are expected to be inherently free of internal electrostatic fields along the growth direction. In fact, we have found various indications for this expectation, none of which are conclusive by themselves, but when taken together, provide persuasive evidence for the absence of these fields. The complex recombination dynamics observed thus directly demonstrates the existence of localized states, and can indeed be consistently described by a simple model taking into account both the relaxation of excitons towards localized states and their spatiotemporal redistribution within the band of localized states. Finally, the higher room-temperature PL intensity of these structures when compared to *M*-plane GaN/(Al,Ga)N MQW's evidences the beneficial role of localization in this materials system even in the absence of internal electrostatic fields.

We are indebted to Manfred Ramsteiner for the Raman measurements and to Lutz Schrottke for a critical reading of the manuscript.

*Electronic address: yjsun@pdi-berlin.de

¹H. M. Ng, Appl. Phys. Lett. **80**, 4369 (2002).

²M. D. Craven, S. H. Lim, F. Wu, J. S. Speck, and S. P. DenBaars, Appl. Phys. Lett. **81**, 469 (2002).

³M. D. Craven, S. H. Lim, F. Wu, J. S. Speck, and S. P. DenBaars, Appl. Phys. Lett. **81**, 1201 (2002).

⁴P. Waltereit, O. Brandt, A. Trampert, H. T. Grahn, J. Menniger, M. Ramsteiner, M. Reiche, and K. H. Ploog, Nature (London) **406**, 865 (2000).

⁵P. Waltereit, O. Brandt, and K. H. Ploog, Appl. Phys. Lett. **75**, 2029 (1999).

⁶Y. J. Sun, O. Brandt, and K. H. Ploog (unpublished).

⁷A. Trampert, T. Liu, P. Waltereit, O. Brandt, and K. H. Ploog, in *Proceedings of the 2001 Microscopy Semiconductor Materials Conference*, IOP Conf. Proc. No. 169 (Institute of Physics, London, 2002), p. 277.

⁸O. Brandt, P. Waltereit, and K. H. Ploog, J. Phys. D **35**, 577 (2002).

⁹O. Brandt, P. Waltereit, S. Dhar, U. Jahn, Y. J. Sun, A. Trampert, K. H. Ploog, M. A. Tagliente, and L. Tapfer, J. Vac. Sci. Technol. B **20**, 1626 (2002).

¹⁰Y. J. Sun, O. Brandt, U. Jahn, T. Y. Liu, A. Trampert, S. Cronenberg, S. Dhar, and K. H. Ploog, J. Appl. Phys. **92**, 5714 (2002).

¹¹B. J. Skromme, J. Jayapalan, R. P. Vaudo, and V. M. Phanse, Appl. Phys. Lett. **74**, 2358 (1999).

¹²K. Kornitzer, T. Ebner, K. Thonke, R. Sauer, C. Kirchner, V. Schwegler, M. Kamp, M. Leszczynski, I. Grzegory, and S. Porowski, Phys. Rev. B **60**, 1471 (1999).

¹³P. Waltereit, O. Brandt, K. H. Ploog, M. A. Tagliente, and L. Tapfer, Phys. Rev. B **66**, 165322 (2002).

¹⁴S. Ghosh, P. Waltereit, O. Brandt, H. T. Grahn, and K. H. Ploog, Phys. Rev. B **65**, 075202 (2002).

¹⁵X. Chen, B. Henderson, and K. P. O'Donnell, Appl. Phys. Lett. **60**, 2672 (1992).

¹⁶J. Z. Li, J. Y. Lin, H. X. Jiang, A. Salvador, A. Botchkarev, and H. Morkoç, Appl. Phys. Lett. **69**, 1474 (1996).

¹⁷H. Scher, M. F. Shlesinger, and J. T. Bendler, Phys. Today **44** (1), 26 (1991).

¹⁸A. Vertikov, I. Ozden, and A. V. Nurmikko, J. Appl. Phys. **86**, 4697 (1999).

¹⁹M. Pophristic, F. H. Long, C. Tran, I. T. Ferguson, and J. R. F. Karlicek, Appl. Phys. Lett. **73**, 3550 (1998).

²⁰J.-C. Holst, A. Hoffmann, D. Rudloff, F. Bertram, T. Riemann, J. Christen, T. Frey, D. J. As, D. Schikora, and K. Lischka, Appl. Phys. Lett. **76**, 2832 (2000).

²¹S. F. Chichibu, M. Sugiyama, T. Onuma, T. Kitamura, H. Nakanishi, T. Kuroda, A. Tackeuchi, T. Sota, Y. Ishida, and H. Okumura, Appl. Phys. Lett. **79**, 4319 (2001).

²²E. O. Göbel and W. Graudszus, Phys. Rev. Lett. **48**, 1277 (1982).

²³J. H. Collet, H. Kalt, L. S. Dang, J. Cibert, K. Saminadayar, and S. Tatarenko, Phys. Rev. B **43**, 6843 (1991).